Silicon (2011) 3:199–205
DOI 10.1007/s12633-011-9099-2

ORIGINAL PAPER

Crystallization and Ability of Hydroxyapatite Formation in Some Trivalent Oxides Containing Na-Ca-Silicate Glass-Ceramics

Saad M. Salman · Samia N. Salama · Hany A. Abo-Mosallam

Received: 15 June 2011 / Accepted: 5 September 2011 / Published online: 5 October 2011

Abstract The formation of glass-ceramics based on Na_2O–CaO-silicates containing P_2O_5 with minor additives of some trivalent oxides (e.g. La, In, Ga, and Al), has been investigated. Different crystalline phases including sodium-orthosilicate containing lanthanum, or aluminum were formed together with $Na_2Ca_2Si_3O_9$, $NaInSi_2O_6$, and $Na_3Ga_2Si_3O_{10}$. The nature and mechanism of HA formed in the glass-ceramics are considered. In general, the presence of trivalent oxides in the glass-ceramics progressively reduced the ability to form a calcium phosphate layer on the surfaces of the materials. The addition of In_2O_3 decreased the crystallization of the hydroxyapatite layer. However, in the presence of either Ga_2O_3 or Al_2O_3 only the amorphous calcium phosphate layer was formed after the immersion of the crystallized specimens in the SBF solution.

Keywords Glasses · Trivalent oxides · Crystallization · Glass-ceramic · Bioactivity

1 Introduction

Bioceramics are considered as potential materials as bone because they can form a direct bond with living bone without the formation of surrounding fibrous tissue [1]. Bonding between the bioactive glass or glass–ceramic and the surrounding tissues takes place through the formation of an hydroxyapatite layer, which is very similar to the mineral phase of bone [2]. The bioglass-ceramic materials are biocompatible, osteoconductive and osteointegrative. These are extensively used as bone filler and bone tissue engineering scaffolds [3].

Bioglass material, based on the Na_2O–CaO–SiO_2–P_2O_5 system, was the first glass composition to be able to form an interfacial bond with living bone after implantation [4]. Despite its beneficial effects on bone healing, the uses of bioactive glasses for bone tissue engineering applications have been limited due to their relatively poor mechanical properties in particular low fracture toughness and they are not suitable for load bearing applications [5]. In order to improve the mechanical reliability of glass based biomedical devices, various approaches have been proposed, such as the production of sintered bodies or the deposition of coatings. The well-known bioactive glass 45S5 shows sodium–calcium–silicate type crystals upon thermal treatment. Most often the crystals have been reported as $Na_2Ca_2Si_3O_9$ [6]. Sodium–calcium–silicate crystals have been found to show solid solubility, thus complicating the analysis of the exact composition [7].

The glass-ceramic materials in the system Na_2O–CaO–SiO_2–P_2O_5 have a high mechanical strength and good implantation results [8]. The addition of an intermediate oxide in glass compositions influence the properties of the glasses due to their possible existence in different oxidation states [9]. Schwickest et al. [10] reported that the addition of La_2O_3 and Y_2O_3 led to an increase of the mechanical strength and melting point of the glasses, whereas Cr_2O_3 and Al_2O_3 reduce their surface tension. The substitution of M_2O_3 for CaO in the binary CaO–SiO_2 glass composition progressively reduces the ability to form a calcium phosphate layer on the surfaces exposed to simulated body fluid (SBF) [11].

Singh et al. [12] investigated the influence of the intermediate oxides on bioactivity and structural properties of calcium borosilicate glasses. They reported that the addition of

S. M. Salman · S. N. Salama · H. A. Abo-Mosallam (✉)
Glass Research Department, National Research Centre,
Dokki,
Cairo, Egypt
e-mail: abo-mosallam@hotmail.com

Y_2O_3 and Cr_2O_3 increases the compactness of the glass matrix and leads to crystallization of the hydroxyapatite layer during *in vitro* testing. While, Al_2O_3 and La_2O_3 containing glasses could not form the crystalline HA layer even after 25 days of soaking in SBF with decreasing band gap. Al-Haidary et al. [13] studied the effect of yttria addition on the mechanical, physical and biological properties of bioactive MgO–CaO–SiO_2–P_2O_5–CaF_2 glass-ceramic. They reported that the bioglass-ceramics modified with the addition of Y_2O_3 has an almost almost two-fold increase in hardness, i.e. about 200%.

The aim of the present study is to investigate the effect of adding M_2O_3 (M = In, La, Ga and Al) on the crystallization process and *in vitro* bioactivity behaviour of the glass-ceramics in the system $Na_2Ca_2Si_3O_9$–P_2O_5. The bioactivity of the glass-ceramic samples after the immersion in the simulated body fluid SBF solution was analyzed by EDX/SEM and TF-XRD.

2 Experimental Procedure

2.1 Materials Preparation

The glasses were prepared in five different compositions by taking the starting materials as reagent grade ammonium dihydrogen phosphate ($(NH_4)H_2.PO_4$), calcium carbonate ($CaCO_3$), sodium carbonate (Na_2CO_3) and, quartz (SiO_2), in the required stoichiometric ratio in weight%. Minor additives of lanthanum oxide (La_2O_3), indium oxide In_2O_3, gallium oxide Ga_2O_3, and aluminum oxide (Al_2O_3), were added for each over the weight percent of the base glass oxides (Table 1). The glasses were prepared by melting the starting materials in a Pt-2% Rh crucible at the 1250–1350 °C temperature range in air for 2 h. The homogeneity of the melts was achieved by stirring the melt several times at about 30 min intervals. The melt was cast into rods and as buttons, which were then properly annealed at 450–500 °C for 1 h and left to cool down slowly overnight inside the muffle furnace to minimize the strain.

The progress of crystallization in the glasses was followed by using double stage heat-treatment regimes. The glasses were first heated according to the DTA results at the endothermic peak temperature for 5 h, which was followed by another thermal treatment at the exothermic peak temperature for 10 h duration.

2.2 Material Characterization

2.2.1 Differential Thermal Analysis (DTA)

The thermal behaviour of the finely powdered glass samples was examined using a SETARAM Labsys ^{TM}TG-DSC16. The powdered samples were heated in a Pt-holder against another Pt-holder containing Al_2O_3 powder as a standard material. A uniform heating rate of 10 °C/min was adopted up to the appropriate temperature of the glasses. The results obtained were considered as a guide for determining the heat-treatment temperatures required to induce crystallization in the glasses.

2.2.2 X-ray Diffraction (XRD)

The X-ray powder diffraction (XRD) patterns were recorded using a Bruker AXS D8 Advance X-ray diffractometer (40 kV, 20 mA) from 3º to 80º in steps of 0.01º. The Cu Ka radiation with Ni filtered was used for the X-ray analysis. The reference data for the interpretation of the X-ray diffraction patterns were obtained from ASTM X-ray diffraction card files.

2.3 Bioactivity (*In Vitro*) Characterization

In vitro bioactivity tests all the crystallized specimens were carried out in polyethylene containers by soaking the samples at 37±0.5 °C, for 28 days in 50 ml of Tris-buffered simulated body fluid (SBF) solution. The preparation of SBF was carried out according to the method proposed by Kokubo et al. [14]. The reagents shown in Table 2 were dissolved in deionised water, to prepare 1 liter of SBF solution. The solution was buffered to pH 7.4 with Tris-(hydroxymethyl)-aminomethane $[(CH_2OH)_3CNH_3]$ and hydrochloric acid. The crystalline samples were

Table 1 The composition and DTA analysis data of the glasses studied

Sample No.	Glass oxides (Wt.%)				Minor additives in g over weight percent of glass oxides				DTA	
	Na_2O	CaO	P_2O_5	SiO_2	La_2O_3	In_2O_3	Ga_2O_3	Al_2O_3	T_g	T_c
G_1	16.61	30.05	5.02	48.32	–	–	–	–	600	748
G_2	16.61	30.05	5.02	48.32	4	–	–	–	609	768
G_3	16.61	30.05	5.02	48.32	–	4	–	–	618	761
G_4	16.61	30.05	5.02	48.32	–	–	4	–	582	722
G_5	16.61	30.05	5.02	48.32	–	–	–	4	594	743

T_g = Transition temperature

T_c = Crystallization temperature

Table 2 Ions concentration (mM) in the simulated body fluid (SBF) and human blood plasma

Occurrence	Ions Concentrations (mM)							
	Na^+	K^+	Mg^{2+}	Ca^{2+}	Cl^-	HCO_3^-	HPO_4^{2-}	SO_4^{2-}
Human Plasma	142.0	5.0	1.5	2.5	103.0	27.0	1.0	0.5
(SBF)	142.0	5.0	1.5	2.5	148.8	4.2	1.0	0.5

removed from the SBF, and dried at room temperature. The surface of the dried samples was analyzed by Thin-Film X-ray Diffraction (TF-XRD) (Panalytical, X'Pert Pro, The Netherlands), employing Ni-filtered Cu Kα radiation at 45 Kv and 40 mA. and (SEM-EDX) (JEOL JXA-840A, Electron probe micro-analyzer, Japan) to detect the formation of the HCA layer.

3 Results and Discussion

3.1 Crystallization Characteristics

Several criteria predicting the role of oxides are available. McMillan [15] found that the network modifier cations have ionic field strength $Z/r^2 < 5\,Å^{-2}$. The radius, the coordination number and the ionic field strength of the cations are reported in Table 3 [16, 17]. In Fig. 1 and Table 1 different glass transformation temperature (T_g) trends are observed depending on the type of trivalent oxides added. T_g linearly increases with the addition of lanthanum and indium. However, non-linear trends are observed in the case of Ga_2O_3 and Al_2O_3 containing glasses. T_g is a structural sensitive parameter and it depends on the density of covalent cross-linking and the number and strength of cross-links between the cation and oxygen atoms [18]. This can be explained on the basis that Al^{3+} and Ga^{3+}can act as network forming ions and La^{3+} and In^{3+} as network modifying ions. When a cation enters the structure as a network modifying ion, a mean coordination number close to one in the pure oxide structure should be expected (Table 3). Therefore, according to Ray [18], greater values of T_g would be expected with the addition of La^{3+} and In^{3+} than with Al^{3+} and Ga^{3+} ions. Aluminum and gallium ions enter the silicate glass structure as network forming ions, that is in fourfold coordination [19].

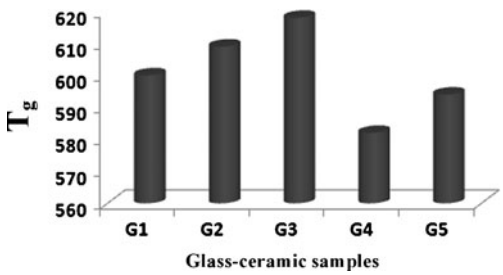

Fig. 1 T_g trend for the glasses with M_2O_3 addition

The progress of crystallization in the glasses, the type and proportions of the resulting crystalline phases were markedly dependant on the glass compositions and the crystallization parameters used. The X-ray diffraction analysis (XRD) (Fig. 2, Pattern I) indicated that the base glass (G_1) formed only sodium calcium silicate solid solution phase, as indicated from the shift of d-spacing lines of (XRD) characteristics for the $Na_2Ca_2Si_3O_9$ phase towards higher 2θ values (major lines 7.55, 4.41, 3.38, 3.33, 2.67, 2.62, 1.87, Card No.22-1455). Guanabara [20] reported that the system Na_2O-CaO-SiO_2 has a tendency to form sodium calcium silicate-$Na_2Ca_2Si_3O_9$ as the main phase. However no crystalline phosphate phase could be detected in glass-ceramic sample G_1 (Fig. 2 pattern I). This indicated that the phosphorus ions may be accommodated in the structure of $Na_2Ca_2Si_3O_9$ to form a solid solution phase after normal two-step heat treatments as discussed in the literature [21, 22].

La_2O_3, In_2O_3 Ga_2O_3 and Al_2O_3 were introduced in the base glass G_1 (as 4 g) over weight percent of glass oxides. Detailed study for the effect of M_2O_3 additions on the crystal phase constitutions developed in the glass-ceramic materials (G_2–G_5) was detected by the X-ray diffraction analysis (XRD) (Fig. 2).

The X-ray diffraction analysis (Fig. 2, Pattern II) revealed that glass G_2 heated at 610 °C/5 h–770 °C/10 h, crystallized into $Na_2Ca_2Si_3O_9$ ss as a major phase together with minor amount of $NaLaSiO_4$ (lines 5.67, 4.72, 3.19, 2.87, 2.83, 2.30, Card No.20-1116). However, the addition of In_2O_3 i.e., G_3 crystallized at 620 °C/5 h–760 °C/10 h, to form $Na_2Ca_2Si_3O_9$ solid solution together with $NaInSi_2O_6$

Table 3 Coordination number in the oxide, CN, radius, r and ionic field strength of the cations, Z/r^2

Cation	CN	r(Aº)	Z/r^2 [$Å^{-2}$]
Si (+4)	4	0.42	22.7
Al (+3)	6	0.51	11.53
Ga (+3)	6	0.62	7.80
In (+3)	6	0.81	4.57
La (+3)	7	1.02	2.90
Ca(+2)	8	1.12	2.04
Na(+1)	8	1.18	0.72

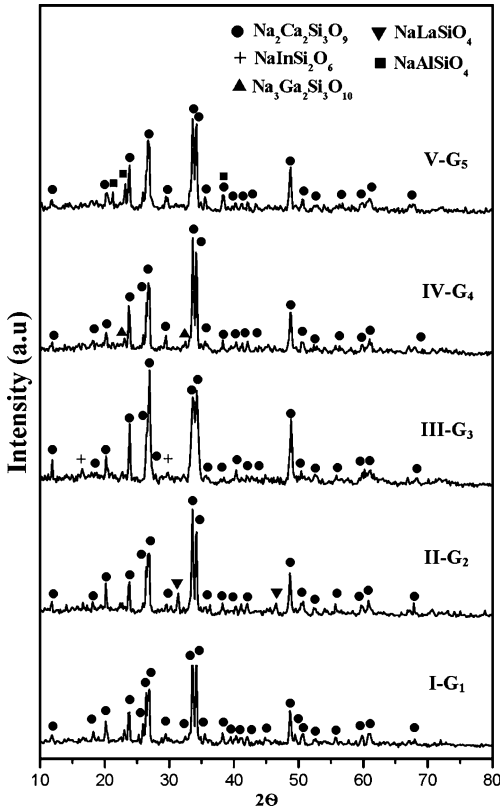

Fig. 2 XRD analysis of the crystallized glasses

phase (lines 6.56, 3.06, 2.98, 2.62, 2.53, Card No.80-929) (Fig. 2, Pattern III). $NaInSi_2O_6$ phase is one of mineral phases of the pyroxene family. Pyroxene is a group of minerals of variable compositions, which crystallize fairly readily. They are closely related in crystallographic and other physical properties as well as in chemical composition, though they crystallized into two crystal systems; orthorhombic and monoclinic [23].

In the case of Ga_2O_3-containing glass (i.e. G_4), the X-ray diffraction analysis (XRD) (Fig. 2, Pattern IV), revealed that the crystallized sample form combeite solid solution ($Na_2Ca_2Si_3O_9$) together with $Na_3Ga_2Si_3O_{10}$ phase (major lines 3.83, 2.98, 3.00, 2.50, Card No. 80–929). With the addition of Al_2O_3 oxide, i.e. G_5 treated at 595 °C/5 h–745 °C/10 h, the nepheline phase ($NaAlSiO_4$) (major lines 4.32, 4.17, 3.83, 3.27, 3.00, 2.88, Card No. 35–424) could be formed (Fig. 2, Pattern V). Nepheline ($NaAlSiO_4$) is a naturally occurring mineral present in silica poor rocks. The nepheline containing ceramics proved to be reliable and suitable for the use in biomedical applications [24].

3.2 Bioactivity

It has been stated that two processes, i.e. dissolution and precipitation, can occur during the soaking of a bioactive materials in simulated biological fluid, leading to the formation of a calcium phosphate layer on the surfaces of the sample. The mechanisms of the calcium phosphate precipitation have been thoroughly discussed in the literature [25]. Briefly, when implant materials are exposed to SBF solution, calcium ions are released from them and silanol groups are formed on their surfaces. The formed silanol groups seem to induce heterogeneous nucleation of apatite. Moreover, the released calcium ions increase the degree of super saturation by increasing the ionic activity product of apatite and accelerate apatite nucleation. Once apatite nuclei are formed, they grow spontaneously, since body fluid and SBF solutions are supersaturated with respect to apatite even under normal conditions [26].

The EDX spectrum of G_1 (free of M_2O_3) and G_2 (with lanthanum) reveals the gradual development of hydroxycarbonate apatite on the surface of the glass-ceramics sample after immersion in SBF solution (Fig. 3). The spherical particles observed in the samples treated in SBF for 28 days are made up of calcium and phosphorus with a Ca/P molar ratio (calculated from EDX analysis) of ~1.67, which is close to the value in HA. Microanalysis of the precipitates reveals the presence of small quantities of Na and Cl as shown in the EDX spectra in Fig. 3. This finding is in agreement with reports given by Dorozhkin et al. [27] which claim that the growth of HA in SBF is accompanied by the incorporation of sodium, magnesium and chlorine ions as well.

The scanning electron micrographs provide visual evidence of the formation of a surface layer on the bioglass-ceramics, which can be presumed to be an apatite layer. After 28 days of immersion in SBF solution, the whole surface of G_1 and G_2 specimens was covered with spherical Ca–P particulate apatite layer (Fig. 3). Since the sintered 45S5 Bioglasss material is in fact a glass–ceramic, one might argue that the bioactivity of the sintered material could be attributed to the residual glass phase. Chen et al. [28] suggested that the bioactivity remains also with the crystalline phase $Na_2Ca_2Si_3O_9$, based on two reasons: (1) the bioactivity of the pure $Na_2Ca_2Si_3O_9$ phase has been reported [21], and (2) the transition from $Na_2Ca_2Si_3O_9$ to an amorphous phase provides an explanation for the finding that the presence of $Na_2Ca_2Si_3O_9$ decreased the kinetics of apatite formation but did not inhibit the growth of an apatite layer on the form surfaces, which has been reported in the literature [29]. On the other hand, the high bioactivity of G_1 and G_2 may be attributed to the formation of $Na_2Ca_2Si_3O_9$ solid solution by accommodated P_2O_5 in its structure. The state of phosphorus ions affects the bioactivity: glass ceramics containing a crystalline phosphate phase are less reactive than that containing phosphorus present in solid solution [21], therefore the dissolution behaviour and bioactivity are decreased.

TF-XRD patterns of the controlled heat treated glasses after immersion in the SBF for 28 days are shown in Fig. 4.

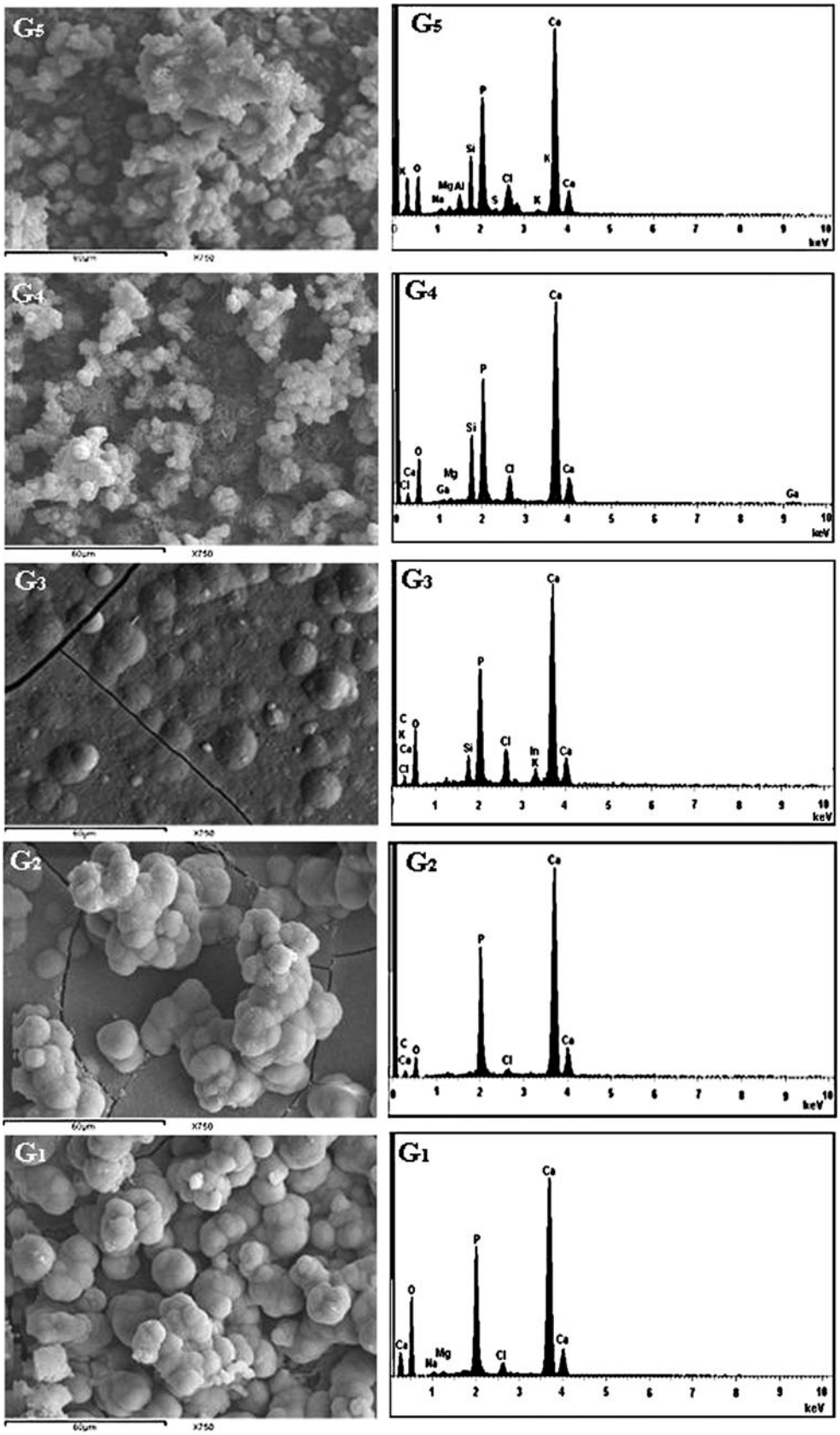

Fig. 3 SEM micrographs and EDAX spectra of the crystallized samples after immersion in SBF solution for 28 days

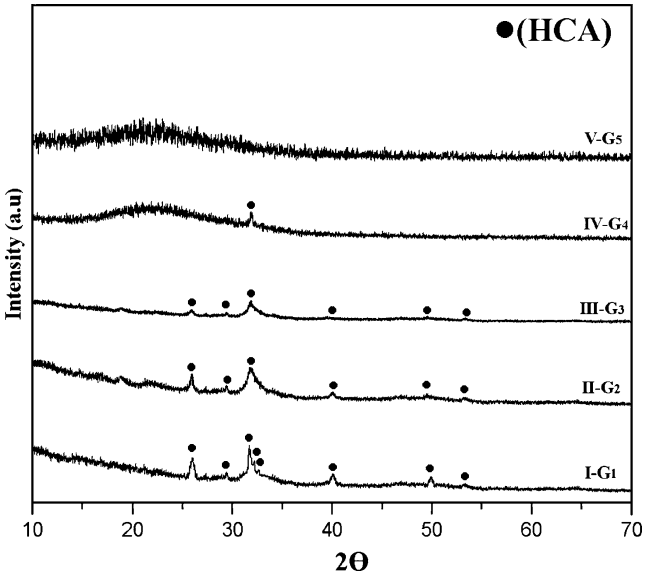

Fig. 4 TF-XRD analysis of crystallized glasses after immersion in SBF solution for 28 days

The patterns of the crystallized samples, G_1 and G_2, indicated the formation of a crystalline apatite layer on their surfaces after 4 weeks of immersion in the SBF solution. The typical crystalline diffraction pattern of hydroxyapatite can be observed with peaks at d-spacing values of 3.46 Å, 2.78 Å, 2.68 Å, 2.62 Å and 2.23 Å, (matched with ICSD card number 19-272). These diffraction peaks were sharper for G_1 than G_2, indicating a higher crystallinity of apatite layer was formed.

The EDAX analysis of the surface of the crystalline specimen G_3 soaked in SBF solution for 28 days is presented in Fig. 3. The crystalline sample showed significant peaks of calcium, phosphorous and a short peak for silica. The results indicated that the presence of In_2O_3 in the glass, led to reduce the thickness of the calcium phosphate layer as compared with the apatite layers formed on the surface of glass-ceramic samples G_1 and G_2. This may be attributed to the field strength of the In^{3+} ion, which is higher than the field strength of the other glass network modifier cations entering the glass [30]. The greater the ionic field strength of the In_2O_3 should increase the acidity of the silanolic group which inhibits or retards the precipitation of the calcium phosphate layer [11].

The size of the apatite crystals at the surface of the crystalline sample G_3 after immersion in the SBF solution are smaller than the size of the hydroxyapatite formed at the surface of the glasses G_1 and G_2 Fig. (3). This may be attributed to the presense of In_2O_3 which may be retarded the formation of the apatite layer on the crystalline sample containing indium oxide. The size of the HA crystalline layer depends on the rate of crystal growth on the surface of the glass-ceramic subjected to the SBF solution. The variation of the crystallite size with immersion time shows a sharp increase in crystallite size of the apatite layers [31]. Figure 4 shows the TF-XRD pattern obtained from the surfaces of glass-ceramic G_3 with In_2O_3 after immersion in SBF for 28 days. It was found that broad peaks of hydroxyapatite (HA) appearing in this sample may be due to the presence of small sized crystallites apatite layer. The results are in good agreement with those reported in the literature [32].

The EDAX spectra detected from sample G_4 (with Ga_2O_3) after immersion in SBF solution showed significant peaks of calcium, phosphorous and a short peak for Mg, Si, and Ga. Similar traces were also detected from the pattern of G_5 (with Al_2O_3) except an Al peak which could be detected instead of a Ga peak as shown in Fig. 3. This may be due to the formation of apatite layers on the surfaces of these samples**.** Also the scanning electron micrograph (Fig. 3) of the immersed crystalline samples G_4 and G_5 showed the formation of amorphous layers on the surfaces of the crystallized specimens. The amorphous phase detected by SEM after the immersion (Fig. 3) represents the amorphous calcium phosphate, as shown by Hench and Wilson [33].

There was another evidence to confirm the formation of amorphous apatite layer on the surfaces of the crystalline samples G_4 and G_5 sought by using the thin film X-ray diffraction (TF-XRD). Figure 4 shows the TF-XRD patterns of the G_4 and G_5 glass-ceramics, containing constant amounts of Ga_2O_3 and Al_2O_3, respectively, after soaking in SBF for 28 days, and no peaks could be observed in the patterns of these specimens which indicated the presence of the amorphous apatite layer. The formation of amorphous HA layers may be attributed to the addition of Ga_2O_3 and Al_2O_3 to the glasses which led to a decrease in the dissolution and the bioactivity rates of its crystalline samples. Hench and Wilson [33] indicated that the addition of small amount of multivalent elements such as Al^{3+}, Zr^{4+} and Ta^{5+} to either bioactive glasses or glass-ceramics decrease the bioactivity. The addition of small amounts of Al_2O_3 [34] and Ga_2O_3 [11] in the starting glass composition decreased the kinetics of apatite layer formation.

4 Conclusion

The influence of some trivalent oxides including La_2O_3, In_2O_3, Ga_2O_3 and Al_2O_3 on the crystallization, nature and mechanism of hydroxyl apatite formed in sodium calcium phosphorus silicate glass-ceramics were investigated. Varieties of silicate crystalline phases could be formed depending on the compositional variation of the glasses. Combeite ($Na_2Ca_2Si_3O_9$), $NaLaSiO_4$, $NaInSi_2O_6$ $Na_3Ga_2Si_3O_{10}$ and $NaAlSiO_4$ phases were crystallized by controlled heat-treatment of the glasses.

The addition of intermediate oxides plays an important role in determining the bioactive behaviour of the crystallized glasses. Generally the addition of the trivalent oxides progressively reduces the ability to form a calcium phosphate layer on the sample surfaces. The addition of In_2O_3 led to a decrease of the crystallization of the hydroxyapatite layer. However in the presence of either Ga_2O_3 or Al_2O_3 in the glasses only amorphous calcium phosphate layer could be formed after the immersion of the crystallized specimens in the SBF solution.

Acknowledgments The authors would like to thank the National Research Centre, Dokki, Cairo, Egypt for the facilities provided.

References

1. Sainz MA, Pena P, Serena S, Caballero A (2010) Influence of design on bioactivity of novel $CaSiO_3$–$CaMg(SiO_3)_2$ bioceramics: in vitro simulated body fluid test and thermodynamic simulation. Acta Biomaterial 6:2797–2807
2. Vitale-Brovarone C, Verné E, Robiglio L, Martinasso G, Canuto RA, Muzio G (2008) Biocompatible glass-ceramic materials for bone substitution. J Mater Sci Mater Med 19:471–478
3. Chen QZ, Efthymiou A, Salih V, Boccaccini AR (2008) Bioglass-derived glass-ceramic scaffolds: study of cell proliferation and scaffold degradation in vitro. J Biomed Mater Res A 84:1049–1060
4. Hench LL (2006) The story of bioglass. J Mater Sci Mater Med 17:967–8
5. Dieudonne SC, Van den Dolder J, de Ruijter JE, Paldan H, Peltola T, Van MA, Hof T, Happonen RP, Jansen JA (2002) Osteoblast differentiation of bone marrow stromal cells cultured on silica gel and sol–gel-derived titania. Biomaterials 23:3041–3051
6. Arstila H, Vedel E, Hupa L, Hupa M (2007) Factors affecting crystallization of bioactive glasses. J Eur Ceram Soc 27:1543–1546
7. Karlsson KH, Backman R (2005) In: Pye LD, Montenero A, Joseph I (eds) Properties of glass-forming melts. Taylor & Francis, Boca Raton, FL, p 11
8. Lin F, Hon M (1988) A study on bioglass ceramics in the Na_2O–CaO–SiO_2–P_2O_5 system. J Mat Sci 23:4295–4299
9. Lahl N, Singh K, Singheiser L, Hilpert K (2000) Crystallization kinetics in AO-AbO_3-SiO_2-B_2O_3 glasses. J Mat Sci 35:3089–3096
10. Schwickest T, Sievering R, Geasee P, Conradt R (2002) Glass ceramic materials as sealants for SOFC applications. Mat-wissu Werkstofftech 33:363–366
11. Branda F, Arcobello-Varlese F, Costantini A, Luciani G (2002) Effect of the substitution of M_2O_3 (M=La, Y, In, Ga, Al) for CaO on the bioactivity of 2.5CaO $2SiO_2$ glass. Biomaterials 23:711–716
12. Singh K, Bala I, Kumar V (2009) Structural, optical and bioactive properties of calcium borosilicate glasses. Ceram Int 35:3401–3406
13. Al-Haidary J, Al-Haidari M, Qrunfuleh S (2008) Effect of yttria addition on mechanical, physical and biological properties of bioactive MgO–CaO–SiO_2–P_2O_5–CaF_2 glass ceramic. Biomed Mater 3:1500–1505
14. Kokubo T, Kushitani H, Yamamuro T (1990) Solutions able to reproduce in vivo surface-structure changes in bioactive glass-ceramic A-W. J Biomed Mater Res 24:721–34
15. McMillan PW (1979) Glass-ceramics. Academic Press, London
16. Weast RC (1977–1978) CRC handbook of chemistry and physics, 58th ed., CRC, Ohio
17. Rawson H (1967) Inorganic glass-forming systems. Academic Press, New York
18. Ray NH (1974) Composition property relationships in inorganic oxide glasses. J Non-Cryst Solids 15:423–434
19. Branda F, Arcobello-Varlese F, Costantini A, Luciani G (1999) Tg and FTIR of (2.5 - x)CaO.x/$3M_2O_3$.$2SiO_2$ (M=Y, La, In, Al, Ga) glasses. J Non-Cryst Solids 246:27–33
20. Guanabara P (2004) Bioactivity study of glass-ceramics with various crystalline fractions obtained by controlled crystallization. Mat Sci Eng C 24:689–691
21. Peitl O, Zanotto ED, Hench LL (2001) Highly bioactive P_2O_5–Na_2O–CaO–SiO_2 glass–ceramics. J Non-Cryst Solid 292:115–26
22. Salman SM, Salama SN, Darwish H, Abo-Mosallam HA (2009) In vitro bioactivity of glass–ceramics of the $CaMgSi_2O_6$–$CaSiO_3$–$Ca_5(PO_4)_3$ F–Na_2SiO_3 system with TiO_2 or ZnO additives. Ceram Int 35:1083–1093
23. Deer WA, Howie RA, Zussman (1992) An introduction to the rock forming minerals. Third ELBS impression. Commonwealth, Printing Press Ltd, Hong Kong
24. Radovan D, Vera D, Predrag V, Smilja M, Slobodan M (2004) Structural characterization of pure Na-nephelines synthesized by zeolite conversion route. J Phys Chem Solids 65:1623–1633
25. Balamurugan A, Balossier G, Michel J, Kannan S, Benhayoune H, Rebelo AHS, Ferreira JMF (2007) Sol gel derived SiO_2–CaO–MgO–P_2O_5 bioglass system-preparation and in vitro characterization. J Biomed Mater Res B 83:546–553
26. Ohtsuki C, Kokubo T, Yamammuro T (1992) Mechanism of apatite formation on CaO–SiO_2–P_2O_5 glasses in a simulated body fluid. J Non-Cryst Solids 143:84–92
27. Dorozhkin SV, Dorozhkina EI, Epple M (2003) Precipitation of carbonateapatite from a revised simulated body fluid in the presence of glucose. J Appl Biomater Biomech 1:200–2007
28. Chen QZ, Thompsonb ID, Boccaccinia AR (2006) 45S5 Bioglasss-derived glass–ceramic scaffolds for bone tissue engineering. Biomaterials 27:2414–2425
29. Peitl O, LaTorre GP, Hench LL (1996) Effect of crystallization on apatite layer formation of bioactive glass 45S5. J Biomed Mater Res 30:509–14
30. Constantini A, Fresca R, Buri A, Branda F (1997) Effect of the substitution of Y_2O_3 for CaO on the bioactivity of 2.5CaO·$2SiO_2$ glass. Biomaterials 18:453–458
31. Singh RK, Srinivasan A (2010) Bioactivity of ferrimagnetic MgO–CaO–SiO_2–P_2O_5–Fe_2O_3 glass-ceramics. Ceram Int 36:283–290
32. Ylanen H, Karlsson K, Itala A, Aro HT (2000) Effect of immersion in SBF on porous bioactive bodies made by sintering bioactive glass microspheres. J Non-Cryst Solids 275:107–115
33. Hench LL, Wilson J (1984) Surface-active biomaterials. Science 226:630–636
34. Salama SN, Darwish H, Abo-Mosallam HA (2006) HA forming ability of some glass-ceramics of the $CaMgSi_2O_6$–$Ca_5(PO_4)_3$ F–$CaAl_2SiO_6$ system. Ceram Int 32:357–364